NUCL SCI TECH (2019) 30:112
https://doi.org/10.1007/s41365-019-0633-z

Measurement of the prompt neutron spectrum from thermal-neutron-induced fission in U-235 using the recoil proton method

Tie He[1,2] · Pu Zheng[2] · Jun Xiao[2]

Received: 13 June 2018 / Revised: 29 January 2019 / Accepted: 20 March 2019 / Published online: 11 June 2019

Abstract A measurement of the ^{235}U prompt fission neutron spectrum (PFNS) by the recoil proton method was performed at the Institute of Nuclear Physics and Chemistry, China. Details of the method, which include the calculation and validation of the response matrix, are presented. The PFNS for ^{235}U in the energy range 1–12 MeV, induced by thermal neutrons, was obtained. The measured spectrum in the low-energy region was in good agreement with previous work and the ENDF/B-VII library, except for minor differences. In the high-energy region, however, the relative height of the measured spectrum was greater, and an analysis of the experiment indicated uncertainties of 13% at 10 MeV and 24% at 12 MeV. Experimental results showed that the recoil proton method could be used to measure prompt fission neutron spectra. Some directions for future work are included.

Keywords Prompt fission neutron spectra · Recoil proton method · Response matrix · U-235

1 Introduction

High-accuracy data on prompt fission neutron spectra (PFNS) have traditionally played an important role in nuclear engineering design and technology. Other applications have recently arisen, for example, detection of nuclear materials by both active and passive interrogation methods [1]; unfortunately, the data on PFNS are surprisingly scarce. Taking the familiar fissile isotope ^{235}U as an example, despite its thermal-neutron-induced PFNS having already been extensively studied, there is still active research on this isotope. There are significant discrepancies in the literature [2] in ^{235}U PFNS in the lower and higher energy regions; those in the higher energy region, i.e., above 10 MeV, were also confirmed in integral experiments [3, 4]. Several experimental datasets [5] and the ENDF/B-VII evaluation for the prompt fission spectrum of ^{235}U (n_{th}, f) are shown in Fig. 1; the discrepancies in the high-energy region are apparent, and reactor experiments [6] confirm the ENDF/B-VII evaluation problem. Thus, there is a need for new measurements of ^{235}U PFNS in a pure ^{235}U context. Additional motivation comes from the high uncertainties in the existing PFNS experiments. To clarify these discrepancies, more reliable and accurate fission spectra are necessary. In the previous work, PFNS were mainly measured by neutron time-of-flight (n-TOF) [7–9]. Traditional fission detection has used a fission chamber to analyze the fragments released [10, 11]. However, the TOF technique in PFNS measurements needs a high-powered fission chamber with unambiguous alpha-fission discrimination, excellent time resolution, a low mass of structural material, and a reasonable level of actinides [12]; such a chamber is not commonly available. At the same time, the range of the fission fragments in matter is very small, limiting the

This work was supported by the National Natural Science Foundation of China (No. 11775196) and the Chinese Special Project for ITER (No. 2015GB108006).

✉ Tie He
2013326050003@stu.scu.edu.cn; jjxy_02@aliyun.com

[1] Key Laboratory of Radiation Physics and Technology, Ministry of Education, Institute of Nuclear Science and Technology, Sichuan University, Chengdu 610064, China

[2] Institute of Nuclear Physics and Chemistry, China Academy of Engineering Physics, Mianyang 621900, China

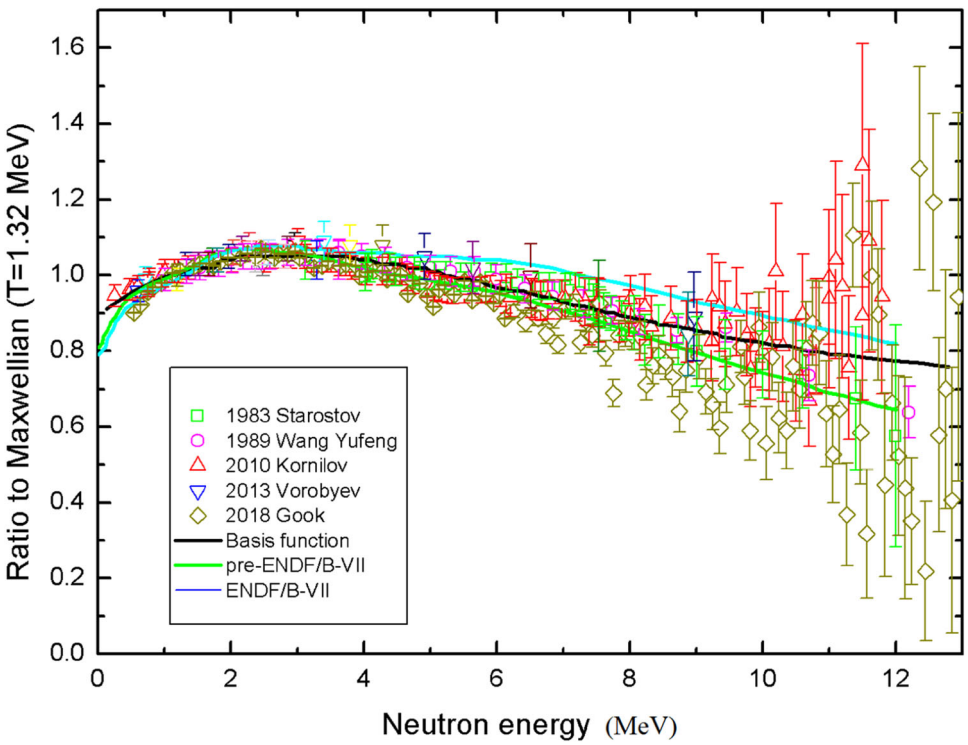

Fig. 1 (Color online) Current experimental data for ^{235}U(n_{th}, f): the prompt fission neutron spectrum, expressed as a ratio to the Maxwellian function for $T = 1.32$ MeV. The basic function and parameters are discussed in [6]

effective sample thickness and therefore also the fissionable mass available for investigation; the small mass leads to a statistically low number of counts in the measured spectra. This is the main reason for the large uncertainty in the high-energy region. Therefore, it is necessary to develop a new method to measure PFNS without a dedicated fission chamber. The recoil proton method [13–15], which is frequently used in neutron physics experiments, could also be used in measurements of the PFNS. This paper presents an investigation of the prompt neutron spectra of thermal-neutron-induced fission in ^{235}U, using the recoil proton method. Technical details of the method, the calculation and validation of the response matrix, and evaluation of the uncertainty are also presented.

2 Recoil proton method [16–18]

The proton method of measuring neutron spectra is based on detecting the proton that recoils when a neutron is elastically scattered in a hydrogenated detector such as a conventional liquid scintillator or one containing stilbene or terphenyl. The energy of the recoil proton E_p is related to the incident neutron energy E_n by the relationship:

$$E_n = \frac{E_p}{\cos^2\theta}, \tag{1}$$

where θ is the angle between the incident neutron and the recoil proton directions. Consequently, the simultaneous measurement of proton energy and recoil angle allows the initial neutron energy to be determined. It can be proved that the distribution of recoil proton energies induced by any single neutron energy is rectangular; the actual proton pulse height spectrum induced by a distribution of neutron energies is then a convolution of the single-energy functions. The incident neutron spectrum is unfolded from the measured recoil proton spectrum by using a detector response function to represent the convolution as

$$\vec{\mathbf{N}} = \mathbf{R}\vec{\Phi}, \tag{2}$$

where $\vec{\mathbf{N}}$ is a vector whose components are the recoil proton pulse spectrum and $\mathbf{R}$ is the response function matrix of the detector, typically obtained from a Monte Carlo simulation such as NRESP [19] or O5S [20]. The vector $\vec{\Phi}$ containing the incident neutron spectrum is then

$$\vec{\Phi} = \mathbf{R}^{-1}\vec{\mathbf{N}}, \tag{3}$$

where $\mathbf{R}^{-1}$ is the inverse of the response function matrix.

3 Experimental

The experiments were carried out in a neutron scattering hall at the Institute of Nuclear Physics and Chemistry (INPC), Mianyang, China; a thermal neutron beam from the 20-MW China Mianyang Research Reactor (CMRR) [21] was used. The experimental layout is shown in Fig. 2.

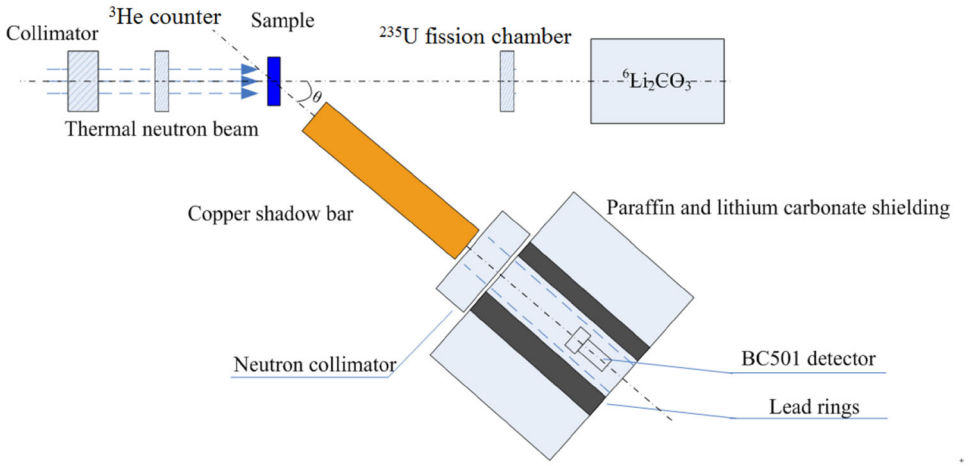

Fig. 2 (Color online) Experimental arrangement for the prompt fission neutron spectrum measurement of $^{235}U(n_{th}, f)$. The copper shadow bar was used only during background measurements

The total neutron flux of the beam for the experiments was about 4×10^6 n s^{-1} cm^{-2}; the measured neutron wavelength was $\lambda = 2$ Å, corresponding to the energy of the thermal neutrons; the beam size at the sample position was 3×5 cm (Fig. 3). The sample was enriched uranium metal with ^{235}U purity above 90%; the sample shape was a cylinder with dimensions Φ25 mm × 0.47 mm; the total mass of ^{235}U was 4 g. A block of neutron-absorbing

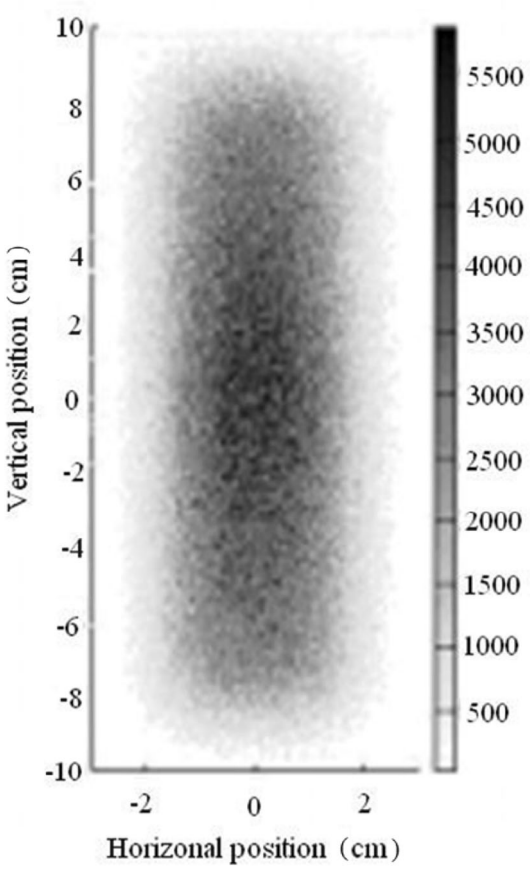

Fig. 3 Distribution of thermal neutron flux at the sample position

$^{6}Li_2CO_3$ material was used as a beam stop after the experimental area. A BC501 liquid scintillation detector was used to acquire the neutron spectrum (main neutron detector, MND); this device has a size of Φ76.2 mm × 50.8 mm and has good linearity, excellent neutron and gamma (n-γ) discrimination, and high light output [22–24]. A further feature of the BC501 liquid scintillator is isotropic response, a significant advantage over solid detectors [25]. The distance between the center of the ^{235}U sample and the BC501 detector was 60 cm. The detector was placed in a massive shield consisting of lead and Li_2CO_3-loaded paraffin, as shown in Fig. 2. The angle (θ) between the axis of the MND and the beam line was 45°. A copper "shadow bar" with dimensions Φ10 cm × 40 cm was placed in front of the MND to reduce the scattered neutron background. A collimating shield of Li_2CO_3 with a tapered inner bore was placed directly in front of the massive main shield surrounding the MND to further reduce background neutron events.

A schematic of the electronics for measuring the prompt fission neutron spectra is shown in Fig. 4. The dynode signal from the MND is fed into a preamplifier (ORTEC 113) and an amplifier (ORTEC 572). The discrimination of neutrons from gammas was realized by a zero-crossing method [20]. The neutron signal was selected by the time-to-amplitude converter (ORTEC 567) and used as coincidence input to a linear gate and stretcher (ORTEC 542); the amplifier (ORTEC 572) output signal was used to record the recoil proton pulse height spectra. Due to the restricted range of linearity of the BC501A scintillator, the proton pulse height spectra were divided into a low-energy region and a high-energy region; the low-energy region was from 0.5 to 3 MeV with a lower threshold setting of 0.4 MeV, while the high-energy region was from 2 to 16 MeV with a lower threshold of 1.75 MeV. The lower energy threshold was set by calculating and adjusting the lower-level discriminator of a timing single-channel analyzer (ORTEC

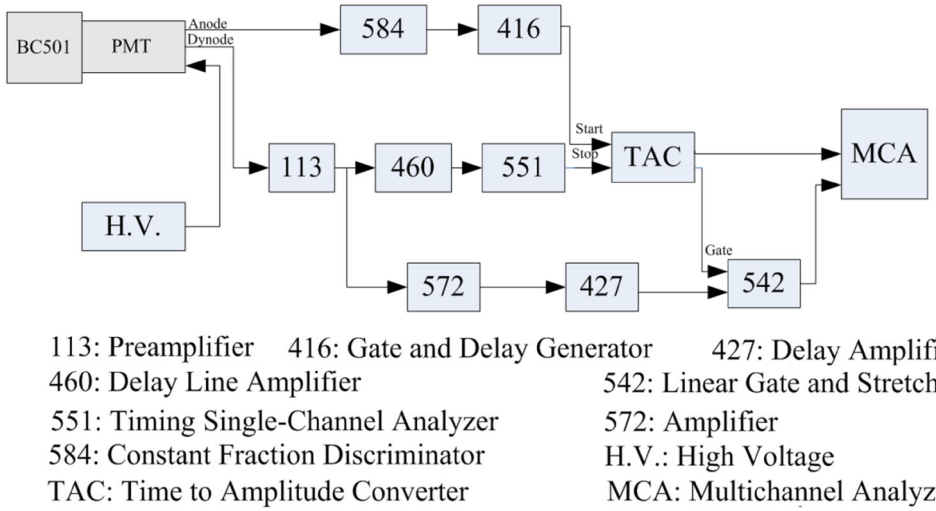

Fig. 4 Electronics schematic for measurement of the fission neutron spectrum. A zero-crossing method is used to discriminate neutrons from gammas

551) accordingly, based on the value of the neutron energy. A standard monoenergetic gamma source (^{22}Na) with the two energies 0.511 (annihilation peak) and 1.274 MeV (gamma decay) was used to calibrate the system for the two energy ranges. The neutron flux was monitored in-line and in real time by two detectors: a ^{3}He proportional counter and a ^{235}U fission chamber; the proportional counter was positioned in the neutron beam upstream of the experiment, while the fission chamber was positioned downstream from the ^{235}U sample. During the course of the experiment, the thermal neutron flux in the beam was held stable; consequently, the two energy regions could be connected and time-normalized to form the complete proton-recoil spectrum. The experimental parameters are summarized in Table 1.

4 Results and discussion

4.1 Response matrix

The proton-recoil spectra are unfolded to obtain the incident neutron energy spectra by using a neutron response matrix; the matrix is derived from the response function for monoenergetic neutrons. Several Monte Carlo codes including O5S [20], SCINEFLU [26], and MCNP [27, 28] have been used to calculate the response functions of liquid scintillators; in this work, we use the software code NRESP7 [19], which was developed at the Physikalisch-Technische Bundesanstalt (PTB) Institute in Germany, to calculate the response function of the BC501 detector. In our analysis, several realistic factors are taken into account: neutron scattering in the aluminum detector housing and in the light pipe, neutron scattering from carbon nuclei, anisotropy of the (n,p) reaction for neutron energy above 10 MeV, and nonlinearities in the light output. For convenience in unfolding the spectra, an energy interval of 0.25 MeV is used. The results of the calculation are shown in Fig. 5. The monoenergetic neutron response functions shown have not been convoluted with the detector resolution, producing a steep edge and a rectangular shape.

To validate the calculated response function, we performed a simple experiment using a D-T neutron source to measure the BC501 detector response. The experiment was carried out at INPC in a spacious experiment hall of length 26 m, width 11 m, and height 14 m. Neutron generation was by the T(d,n) ^{4}He reaction using a 134-keV deuteron beam. The neutron yield was monitored by counting the associated alpha particles with an Au–Si surface-barrier

Table 1 Summary of experimental parameters for the two energy regions

	High-energy part	Low-energy part
Energy range	2–16 MeV	0.5–4.25 MeV
Threshold	1.75 MeV	0.45 MeV
High voltage	–1250 V	–1450 V
Calibration	^{22}Na, E_γ = 0.511 MeV	^{22}Na, E_γ = 1.274 MeV
n-gamma discrimination	Zero-crossing	
Neutron beam	Thermal neutron beam, 4×10^6 n s^{-1} cm^{-2}	
Sample	Enriched uranium, Φ 25 mm × 0.47 mm, 4 g	

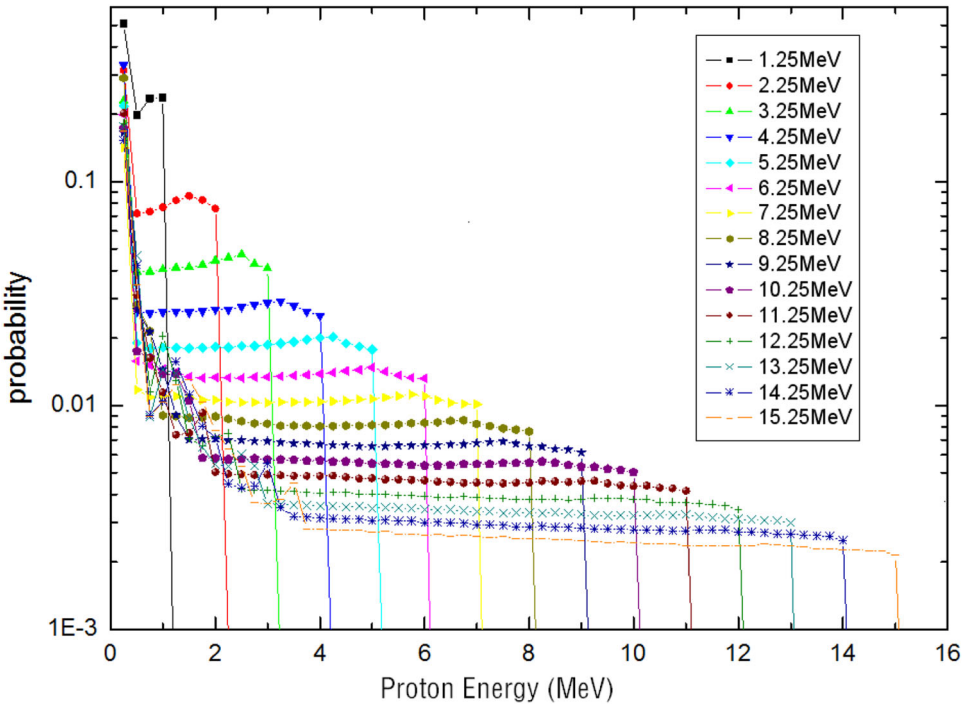

Fig. 5 (Color online) Response functions of the BC501 detector to monoenergetic neutrons (see the legend), calculated by the NRESP7 code

detector located at an angle of 178° from the deuteron beam line. The BC501 detector was placed 10 m away from the D-T source in the 0° direction, where the neutron energy was 14.8 MeV. The measured response function compared with the calculation is shown in Fig. 6. To facilitate comparison with the experiment, the simulated response function was convoluted with the detector resolution. The comparison graph showing the quantity (calculated/experimental-1) is presented in Fig. 7. It can be seen that the calculated response function and the measurement are in good agreement at energies above 4 MeV; however, below 2 MeV, the measured values are higher than calculated. There are two main reasons for the discrepancy: One is the influence of gamma rays. In the

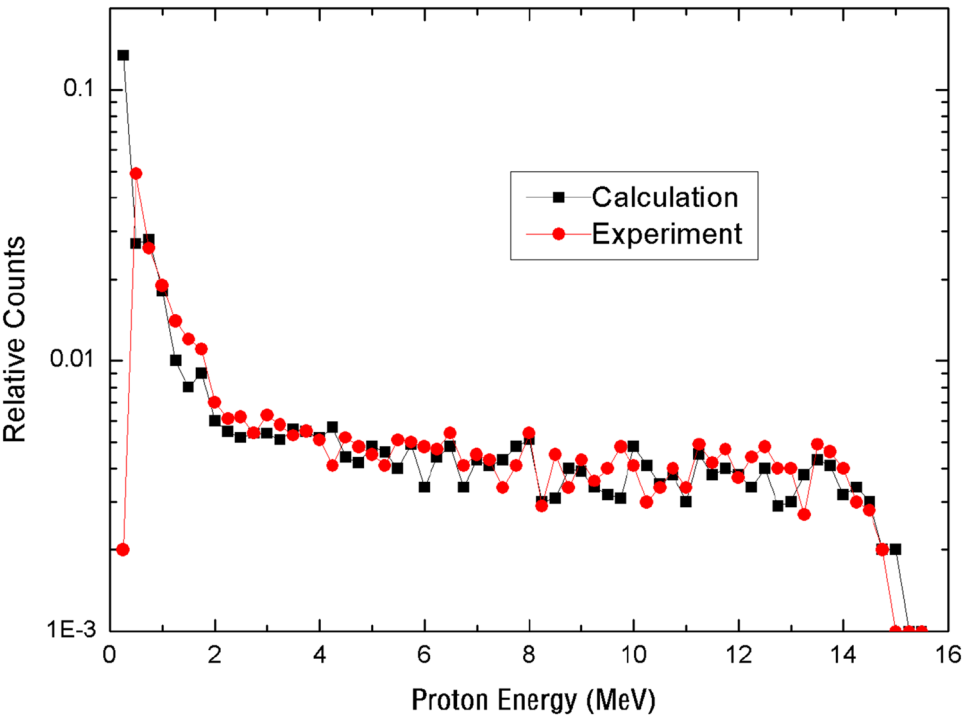

Fig. 6 (Color online) Comparison of response functions: calculated (black rectangles) and experimental (red circles), at an energy of 14.8 MeV

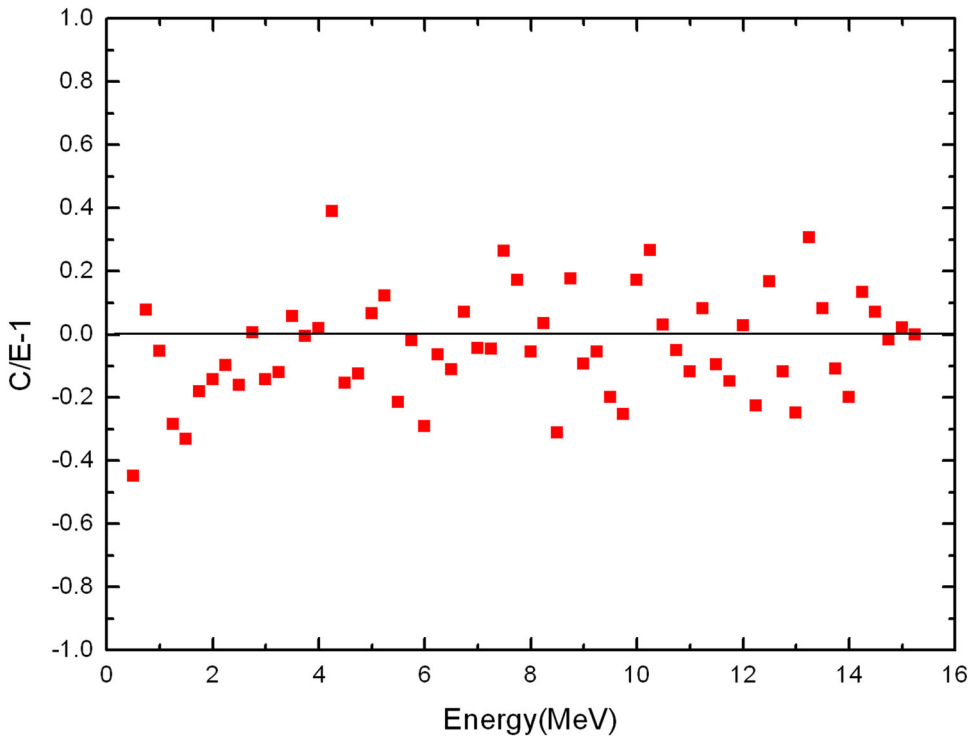

Fig. 7 Comparison of calculated and experimental response functions. The quantity (calculated/experimental-1) is plotted, indicated as (C/E-1)

measurements, the n-γ discrimination in the low-energy region is worse than in the high-energy region. A small fraction of gamma events is recorded as neutron events in the recoil proton spectra, leading to a measured value that is higher than that calculated. A second contributor to the discrepancy is scattered neutrons. Although we have taken several measures to reduce their effect, some scattered neutrons are also recorded in the measured spectra. The recoil proton spectra were unfolded to obtain the incident neutron spectra by the inverse matrix method described above; the results for the D-T neutron source are shown in Fig. 8. The neutron energy of the peak is 14.78 MeV, in good agreement with data from the accelerator manual [29]. It should be mentioned that only one energy (14 MeV) has been experimentally validated, and other experiments will be carried out in the future to improve this situation.

4.2 PFNS and uncertainty

The measurements of the PFNS proton-recoil pulse height spectra were divided into low- and high-energy regions. In the low-energy region, the statistical count level in the recoil proton spectra could be improved, but the measurement time was only several hours. In the high-energy region, as a result of the smaller number of high-energy neutrons, the data took about 50 h to acquire. After the measurements of the source spectra, the background spectra measurement of the two energy segments was carried out using the copper shadow bar described in Fig. 2. It took corresponding amounts of time to complete background spectra measurements in the low- and high-energy regions. The pure or clean recoil proton spectra were obtained by subtracting the background spectra. Based on the recoil proton spectra, the PFNS of $^{235}U(n_{th}, f)$ was obtained using the inverse of the calculated response matrix. The experimental results are summarized in Fig. 9. The ratio of the spectra was obtained by comparing the measured spectra with the Maxwellian function for a temperature $T = 1.32$ MeV, as described in the literature. It can be seen from the figure that the lower threshold in the experimental spectra was set at 1 MeV, limited by the neutron-gamma discrimination for neutron energies below that. Because the uranium sample emitted an elevated level of gamma rays after irradiation by the neutron beam, the n-γ discrimination below 1 MeV was not satisfactory, and in addition, the main parts of the experimental spectra in the low-energy region agreed with the previous work and the ENDF/B-VII library. We believe the small differences are caused by delayed neutrons and scattered neutrons from the uranium sample. While the prompt and delayed neutrons could not be discriminated in the recoil proton method here, we took measures (the copper shadow bar and collimator) to reduce scattered neutrons from the environment; however, scattered neutrons from the uranium sample itself could not be eliminated. In the high-energy region (above 10 MeV), however, our experimental spectrum is higher than the results of Starostov, Wang, Vorobyev, and the

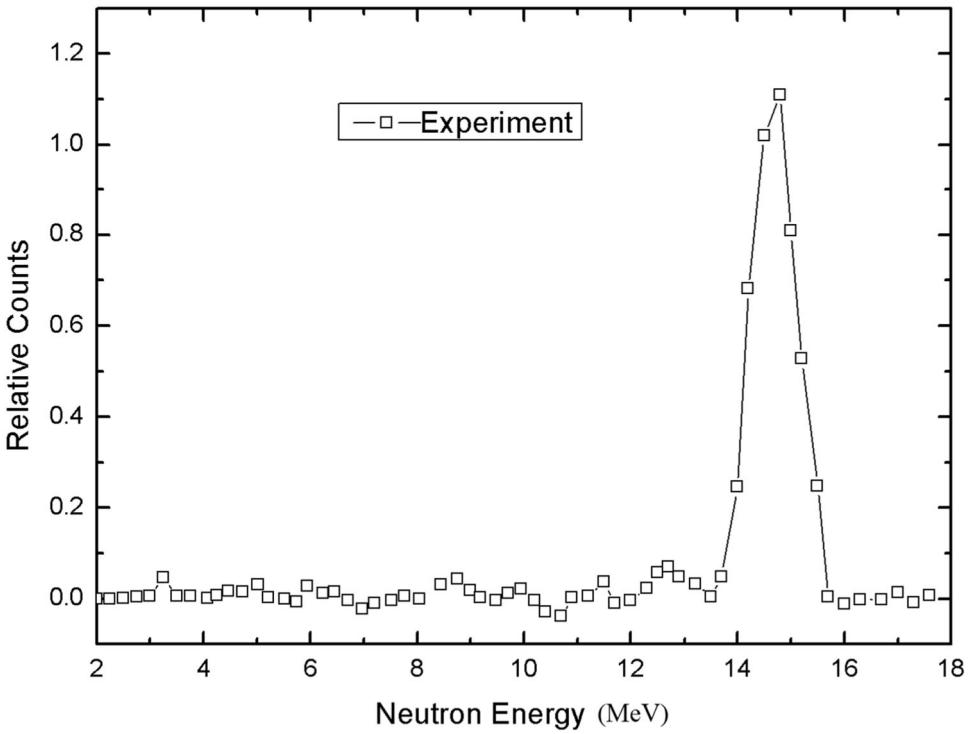

Fig. 8 Spectrum of D-T neutron source, obtained by unfolding measured results using the inverse response matrix

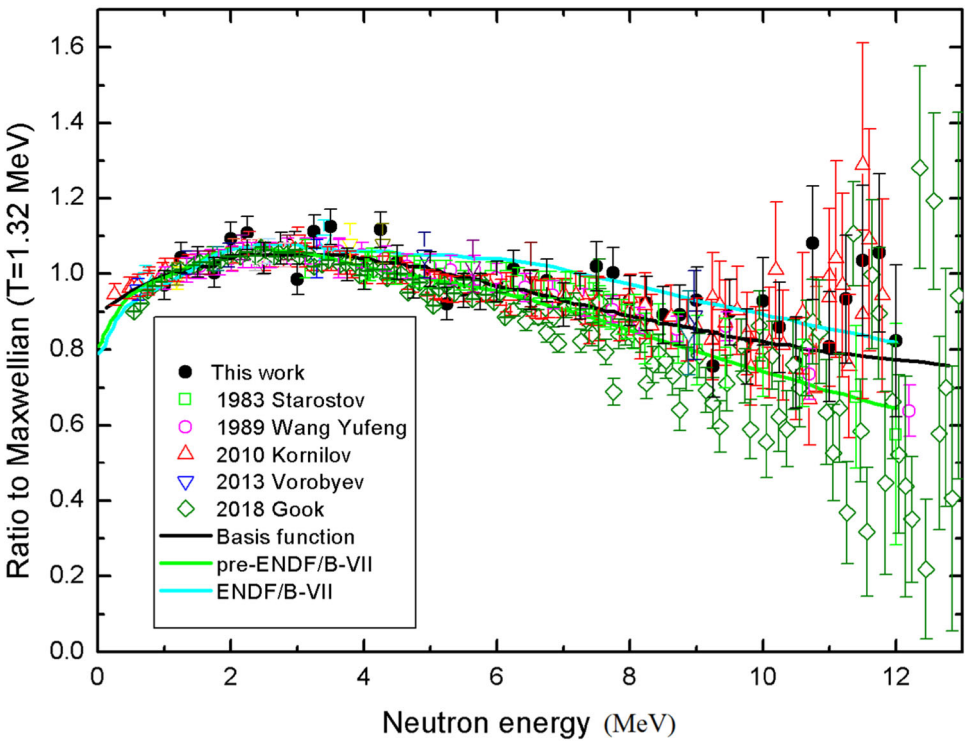

Fig. 9 Experimental spectra of PFNS for $^{235}U(n_{th}, f)$ (black circles) compared with other reports and the ENDF/B-VII library. Comparison with a Maxwellian function for $T = 1.32$ MeV is shown

ENDF/B-VII library. Our results are similar to those of Kornilov, especially if the statistical uncertainties are included. These uncertainties result from, for example, the counting statistics in the recoil proton spectra (σ_1), the calculation of the response matrix (σ_2), the neutron/gamma discrimination (σ_3), and the energy calibration by a standard γ source (σ_4). The statistical uncertainty of the counts is obtained from

$$\sigma_1 = 1/\sqrt{N}, \quad (4)$$

where N is the number of counts in the recoil proton spectra. In our measurement, the statistical uncertainty at 10 MeV is 11%, while the value at 12 MeV is 23%. The uncertainty σ_2 of the response matrix is obtained by the simulated code NRESP7; from the calculations, the relative uncertainty in the low-energy region is 3–4%, while in the high-energy region it is 4–5%. The uncertainty σ_3 of neutron/gamma discrimination above 1 MeV was about 1%. In the high-energy region, the source neutron calibrating spectra contribute an uncertainty σ_4 about 1%, while in the low-energy region, calibrating by a ^{137}Cs source contributes an uncertainty of about 2%. Because the uncertainties in the measurement are independent, the total uncertainty is given by:

$$\sigma_{\text{total}} = \sqrt{\sigma_1^2 + \sigma_2^2 + \sigma_3^2 + \sigma_4^2}. \quad (5)$$

As a result, the total uncertainty in the high-energy region from 10–12 MeV was 13–24%. Although our final uncertainty remains high, it has been reduced considerably relative to some previous work. It can be seen from the uncertainty budget that the greatest contribution to the uncertainty comes from the counting statistics. Consequently, an effective method to reduce uncertainty would be to increase the count numbers by improving the neutron detector's efficiency, using a larger quantity of fissile materials, and extending the measurement duration when machine time permits. In addition, using a neutron source with less energy spread will improve the accuracy of the response function. These are areas we plan to explore in the near future.

5 Conclusion

An experiment was performed to obtain the prompt fission neutron spectrum induced by thermal neutrons in ^{235}U using the recoil proton method. The measured spectrum in the low-energy region is in good agreement with the previous work and with the ENDF/B-VII library except for minor differences. In the high-energy region, however, the measured spectrum is higher in comparison. The uncertainty in the energy region from 10 to 12 MeV is 13–24%, which is an improvement over the previous work. The experimental results show the recoil proton method can be used to measure prompt fission neutron spectra and does not require a dedicated fission chamber.

Acknowledgements We would like to thank Prof. Zhu An from Sichuan University for helpful discussion and Jianming Song and Wei Luo from INPC for providing a high-performance thermal neutron source. We wish to thank Benchao Lou and Yan Li from INPC for providing the D-T neutron source.

References

1. R.C. Haight, H.Y. Lee, T.N. Taddeucci et al., The prompt fission neutron spectrum (PFNS) measurement program at LANSCE. Nucl. Data Sheets **119**, 205–208 (2014). https://doi.org/10.1016/j.nds.2014.08.057
2. R. Capote, A. Trkov, M. Sin et al., IAEA CIELO evaluation of neutron-induced reactions on ^{235}U and ^{238}U targets. Nucl. Data Sheets **148**, 254–292 (2018). https://doi.org/10.1016/j.nds.2018.02.005
3. M. Košt'ál, M. Schulc, V. Rypar et al., Validation of zirconium isotopes (n,g) and (n,2n) cross sections in a comprehensive LR-0 reactor operative parameters set. Appl. Radiat. Isot. **128**, 92–100 (2017). https://doi.org/10.1016/j.apradiso.2017.06.023
4. M. Košt'ál, E. Losa, P. Baroň et al., Measurement of 89Y(n,2n) spectral averaged cross section in LR-0 special core reactor spectrum. Radiat. Phys. Chem. **141**, 22–28 (2017). https://doi.org/10.1016/j.radphyschem.2017.05.027
5. M. Košt'ál, Z. Matěj, E. Losa et al., On similarity of various reactor spectra and ^{235}U prompt fission neutron spectrum. Appl. Radiat. Isot. **135**, 83–91 (2018). https://doi.org/10.1016/j.apradiso.2018.01.028
6. R. Capote, Y.J. Chen, J. Hambschf et al., Prompt fission neutron spectra of actinides. Nucl. Data Sheets **131**, 1–106 (2016). https://doi.org/10.1016/j.nds.2015.12.002
7. A. Enqvist, B.M. Wieger, H. Lu, Neutron-induced ^{235}U fission spectrum measurements using liquid organic scintillation detectors. Phys. Rev. C **86**, 1–10 (2012). https://doi.org/10.1103/PhysRevC.86.064605
8. N. Kornilov, F.J. Hambschf, I. Fabry et al., The ^{235}U(n,f) prompt fission neutron spectrum at 100 K input neutron energy. Nucl. Sci. Eng. **165**, 117–127 (2010). https://doi.org/10.1016/j.NSE.2010.11.008
9. Y.F. Wang, X.X. Bai, A. Li et al., Experimental study of the prompt neutron spectrum of 235U fission induced by thermal neutrons. Chin. J. Phys. **11**, 47–54 (1989)
10. A. Sardet, T. Granier, B. Laurent et al., Experimental studies of prompt fission neutron energy spectra. Phys. Procedia **47**, 144–149 (2013). https://doi.org/10.1016/j.phpro.2013.06.021
11. P. Staples, J.J. Egan, G.H.R. Kegel et al., Prompt fission neutron energy spectra induced by fast neutrons. Nucl. Phys. A **591**, 41–60 (1995)
12. J. Taieb, B. Laurent, G. Belier et al., A new fission chamber dedicated to prompt fission neutron spectra measurements. Nucl. Instrum. Methods A **833**, 1–7 (2016). https://doi.org/10.1016/j.nima.2016.06.137
13. J. Jordanova, L. Olaah, A. Fenyvesi et al., Measurements and calculations of neutron spectra modified by iron slabs bombarded by neutrons with energies up to 14 MeV. Appl. Radiat. Isot. **54**, 307–310 (2001)
14. Y. Chen, L. An, Y.F. Mou et al., Neutronics experiments of Vanadium benchmark. J. Nucl. Sci. Technol. **39**, 1021–1024 (2002). https://doi.org/10.1080/00223131.2002.10875275
15. W.P. Wen, G.W. Li, H.K. Wang, Nuclear emulsion measuring the prompt fission neutron spectrum of ^{238}U induced by 2.8 MeV neutrons. Ann. Nucl. Energy **94**, 576–580 (2016). https://doi.org/10.1016/j.anucene.2016.03.017
16. T. Kajimoto, H. Arakawa, S. Noda et al., Study of recoil-proton-detector system using organic and inorganic scintillators for high energy neutron measurement. J. Nucl. Sci. Technol. **5**, 526–529 (2008). https://doi.org/10.1080/00223131.2008.10875907

17. M. Obu, K. Shirakata, T. Ichimori, Proton-recoil counter technique for measurement of fast neutron spectrum. J. Nucl. Sci. Technol. **16**, 329–343 (1979). https://doi.org/10.1080/18811248.1979.9730909
18. K. Weise, M. Weyrauch, K. Knauf, Neutron response of a spherical proton recoil proportional counter. Nucl. Instrum. Meth. A **309**, 287–293 (1991). https://doi.org/10.1016/0168-9002(91)90114-6
19. G. Dietze, H. Klein, NRESP4 and NEFF4: Monte Carlo codes for the calculation of neutron response functions and detection efficiencies for NE213 scintillation detectors,PTB-ND-22 (1982)
20. R.E. Textor, V.V. Verbinski, O5S: a Monte Carlo code for calculating pulse height distributions due to monoenergetic neutrons incident on organic scintillators, ORNL-4160 (1968)
21. G.A. Sun, C.S. Zhang, B. Chen et al., A new operating neutron scattering facility CMRR in China. Neutron News **27**, 21–26 (2016). https://doi.org/10.1080/10448632.2016.1233018
22. Y.H. Chen, J.R. Lei, X.D. Zhang et al., Study of n-gamma discrimination for 0.4–1 MeV neutrons using the zero-crossing method with a BC501A liquid scintillation detector. Chin. Phys. C **37**, 462021–462024 (2013). https://doi.org/10.1088/1674-1137/37/4/046202
23. M. Nakhostin, P.M. Walker, Application of digital zero-crossing technique for neutron–gamma discrimination liquid organic scintillation detectors. Nucl. Instrum. Methods A **621**, 498–501 (2010). https://doi.org/10.1016/j.nima.2010.06.252
24. T. He, P. Zheng, J. Xiao et al., Benchmark integral neutron experiments for Fe, Be and C with DT neutron by liquid scintillation detector. Appl. Radiat. Isot. **124**, 56–61 (2017)
25. W. Hansen, D. Richter, Determination of light output function and angle dependent correction for a stilbene crystal scintillation neutron spectrometer. Nucl. Instrum. Methods A **476**, 195–199 (2002). https://doi.org/10.1016/S0168-9002(01)01430-9
26. J. Yan, R. Liu, C. Li et al., A comparison of n-gamma discrimination by the rise-time and zero-crossing methods. Sci. China Phys. Mech. **53**, 1453–1459 (2010). https://doi.org/10.1007/s11433-010-4036-8
27. K. Dickens, Scinful: a Monte Carlo based computer program to determine a scintillator full energy response to neutron detector for energy between 0.1 and 80 MeV: user's manual and Fortran program listing, ORNL-6462 (1988)
28. K. Schweda, T.D. Schmidt, Improved response function calculations for scintillation detectors using an extended version of the MCNP code. Nucl. Instrum. Methods A **476**, 155–159 (2002)
29. H.C. Ma, *Accelerator Single-Energy Neutron Source Data Manual in Common Use* (Atomic Energy Press, Beijing, 1976)